

Research Article

Simple One-Pot Synthesis of Hexagonal ZnO Nanoplates as Anode Material for Lithium-Ion Batteries

Haipeng Li,^{1,2,3} Yaqiong Wei,^{1,2,3} Yan Zhao,^{1,2} Yongguang Zhang,^{1,2} Fuxing Yin,^{1,2} Chengwei Zhang,^{1,2} and Zhumabay Bakenov⁴

¹Research Institute for Energy Equipment Materials, Hebei University of Technology, Tianjin 300130, China

²Tianjin Key Laboratory of Laminating Fabrication and Interface Control Technology for Advanced Materials, Hebei University of Technology, Tianjin 300130, China

³School of Material Science & Engineering, Hebei University of Technology, Tianjin 300130, China

⁴Institute of Batteries LLC, Nazarbayev University, Kabanbay Batyr Avenue 53, Astana 010000, Kazakhstan

Correspondence should be addressed to Yongguang Zhang; yongguangzhang@hebut.edu.cn and Zhumabay Bakenov; zbakenov@nu.edu.kz

Received 18 September 2015; Revised 14 December 2015; Accepted 20 December 2015

Academic Editor: Philippe Knauth

Copyright © 2016 Haipeng Li et al. This is an open access article distributed under the Creative Commons Attribution License, which permits unrestricted use, distribution, and reproduction in any medium, provided the original work is properly cited.

Hexagonal ZnO nanoplates were synthesized *via* simple one-pot hydrothermal reaction of $\text{Zn}(\text{CH}_3\text{COO})_2$ and $\text{CO}(\text{NH}_2)_2$. XRD, SEM, and HRTEM were used to investigate the composition and microstructure of the material. Together with the facile strain relaxation during structure and volume change upon cycling, this plate-like structure of ZnO is favorable for physical and chemical interactions with lithium ions because of its large contact area with the electrolyte, providing more active sites and short diffusion distances. The resulting hexagonal ZnO nanoplates electrode exhibited good cyclability and delivered a reversible discharge capacity of 368 mAh g^{-1} after 100 cycles at 0.1 C.

1. Introduction

Lithium-ion batteries (LIBs), the most widely used rechargeable battery for mobile electronic devices, are rapidly expanding their range of applications into fields such as hybrid electrical vehicles (HEV) and electrical vehicles (EV) [1, 2]. This strong market demand stimulates the need for development of advanced lithium-ion batteries with larger specific capacities and higher energy densities. Graphite, owning a low theoretical capacity of 372 mAh g^{-1} , represents the state-of-the-art anode material, which greatly limits the further application of the LIBs [3–5]. This is why, among other promising alternatives, ZnO has been proposed as a more suitable candidate anode for next generation systems based on its much higher theoretical capacity of 978 mAh g^{-1} ; in addition, ZnO has several other advantages, such as low cost, facile preparation, and a high chemical stability [6–8].

Despite these considerable advantages, there are still huge challenges to overcome for ZnO to promote its application in LIBs. Among these is a low reversible capacity, which is

consumed rapidly due to severe volume variations of ZnO particles during the charge/discharge process [9]. Recently, great efforts have been devoted to improve the electrochemical performance of ZnO anodes. Numerous ZnO-based microstructural designs, including porous ZnO [10], ZnO nanofibers [11], and ZnO nanoparticles [12], have been proposed to mitigate the electrode failure due to volume changes. Among various nanostructures, one-dimensional (1D) nanostructures have received considerable attention because the 1D nanostructure is favorable for physical or chemical interactions between the electrodes and lithium ions due to its high surface area and large surface-to-volume ratio, which provides more active sites and short lithium-ion diffusion paths [11].

Herein, we describe a simple one-pot method to synthesize hexagonal ZnO nanoplates by a simple one-pot hydrothermal reaction method. Physical and electrochemical properties of the resultant ZnO as an anode material for LIBs are also reported.

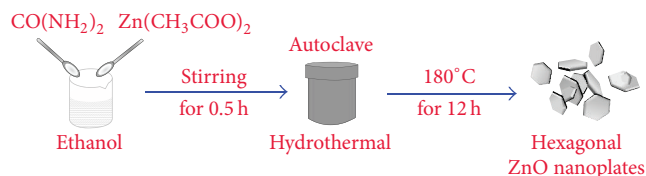


FIGURE 1: Schematics of the preparation of ZnO nanoplates.

2. Experimental

Zinc acetate ($\text{Zn}(\text{CH}_3\text{COO})_2$, $\geq 99\%$), urea ($\text{CO}(\text{NH}_2)_2$, $\geq 99\%$), and ethanol ($\text{CH}_3\text{CH}_2\text{OH}$, $\geq 99.7\%$) were purchased from Tianjin Fuchen Chemical Company and used without further purification. The ZnO preparation is schematically represented in Figure 1. In a typical experiment, 5 mM of $\text{Zn}(\text{CH}_3\text{COO})_2$ and 10 mM of $\text{CO}(\text{NH}_2)_2$ were dissolved in ethanol and stirred for 30 min using a magnetic stirrer. Subsequently, 60 mL of mixture was placed in a 100 mL autoclave at 180°C for 12 h and then cooled to room temperature. The precipitation was alternately centrifuged and washed with distilled water for several times. Finally, the obtained white solid product was dried at 60°C for 24 h in a vacuum oven.

The crystalline phases of the sample were determined by X-ray diffraction (XRD, SmartLab, Rigaku Corporation) equipped with $\text{Cu K}\alpha$ radiation. The sample morphology was examined by scanning electron microscopy (SEM, S-4800, Hitachi Limited). The interior structure of sample was observed using transmission electron microscopy (TEM, JEM-2100F, JEOL) at 160 kV.

The electrochemical performance of sample was investigated using coin-type cells (CR2025). The cell was composed of lithium metal (counter and the reference electrodes) and hexagonal ZnO nanoplate electrode separated by a microporous polypropylene separator soaked in 1 M LiPF_6 in a mixture of dimethyl carbonate/diethyl carbonate/ethylene carbonate (1:1:1 by volume) electrolyte. The ZnO electrode was prepared by mixing 70 wt% as-prepared hexagonal ZnO nanoplate powders, 10 wt% polyvinylidene fluoride (PVDF) (Kynar, HSV900) as a binder, and 20 wt% acetylene black (MTI, 99.5% purity) conducting agent in 1-methyl-2-pyrrolidinone (NMP, Sigma-Aldrich, $\geq 99.5\%$ purity). The resultant slurry was uniformly spread onto nickel foam using a doctor blade and dried at 50°C for 12 h. The resulting anode film was used to prepare the electrodes by punching circular disks with 1 cm in diameter. The active material loading in each electrode was about 2 mg cm^{-2} . The coin cells were assembled in an Ar (99.9995%) filled glove box (MBRAUN) and tested galvanostatically on a multichannel battery tester (BTS-5V5mA, Neware) between 0.005 and 3 V versus Li^+/Li electrode at different current densities.

3. Results and Discussion

XRD analysis measurements were employed to investigate the hexagonal ZnO nanoplates; Figure 2 shows typical XRD patterns of the ZnO sample. XRD pattern is consistent with

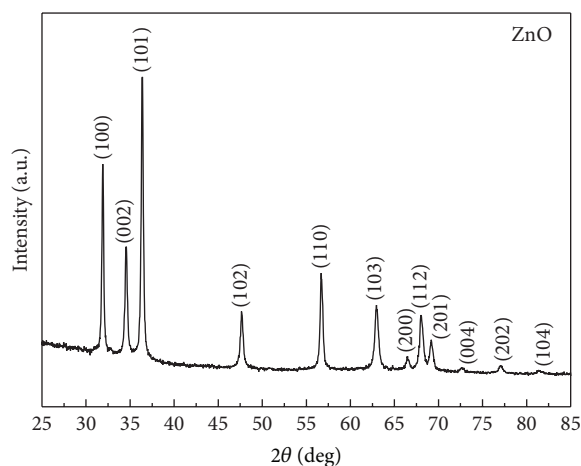


FIGURE 2: XRD patterns of as-prepared ZnO sample.

the JCPDS Card number 36-1451, confirming that a product with the ZnO hexagonal structure with space group $\text{p}63\text{mc}$ and the lattice parameters $a = 0.3257 \text{ nm}$, $c = 0.52156 \text{ nm}$ [10] was successfully synthesized. The XRD peaks at $2\theta = 31.8^\circ, 34.4^\circ, 36.3^\circ, 47.6^\circ, 56.6^\circ, 62.9^\circ, 66.4^\circ, 67.9^\circ, 69.1^\circ, 72.6^\circ, 76.9^\circ,$ and 81.4° could be assigned to (100), (002), (101), (102), (110), (103), (200), (112), (201), (004), (202), and (104) planes of ZnO [13].

The ZnO sample morphology was investigated by SEM (Figure 3(a)). The data confirm as well that hexagonal nanoplates of ZnO were successfully prepared via a simple one-pot hydrothermal reaction of $\text{Zn}(\text{CH}_3\text{COO})_2$ and $\text{CO}(\text{NH}_2)_2$. ZnO was developed with regular nanoplate shapes with an average diameter of around 800 nm and a thickness of around 85 nm; it can be seen that the nanoplates are interconnected, and this may lead to a better electric contact among the active particles [10]. As a result, the electrochemical reactions of the active materials can proceed quicker and more efficiently resulting in an enhanced capacity and high rate capability, as it was confirmed in the following electrochemical tests. Figure 3(b) exhibits the TEM images of ZnO sample showing the formation of hexagonal structured ZnO with a wide range size distribution. At a higher magnification (Figure 3(c)), HRTEM of ZnO sample shows the crystal lattice strips with a measured neighboring interlayer distance of 2.82 \AA , which corresponds to the reported value of interplanar spacing (d_{100}) of (100) lattice plane of hexagonal ZnO phase (JCPDS Card number 36-1451) [14]. This suggestion is in a good agreement with the XRD results showing that the as-prepared ZnO sample is highly crystalline exhibiting strong and sharp reflection peaks, which is further confirmed by HRTEM equipped with the selected area electronic diffraction (SAED). Figure 3(d) shows the corresponding SAED (the single particle in Figure 3(c)) pattern of the sample, indicating that the ZnO nanoplates show a single crystalline structure [15]. Xiao et al. showed that the degree of crystallinity of nanostructured ZnO greatly influences the electrochemical performance of ZnO as anode in lithium-ion batteries, and the specific capacity of ZnO can be improved by enhancing the degree

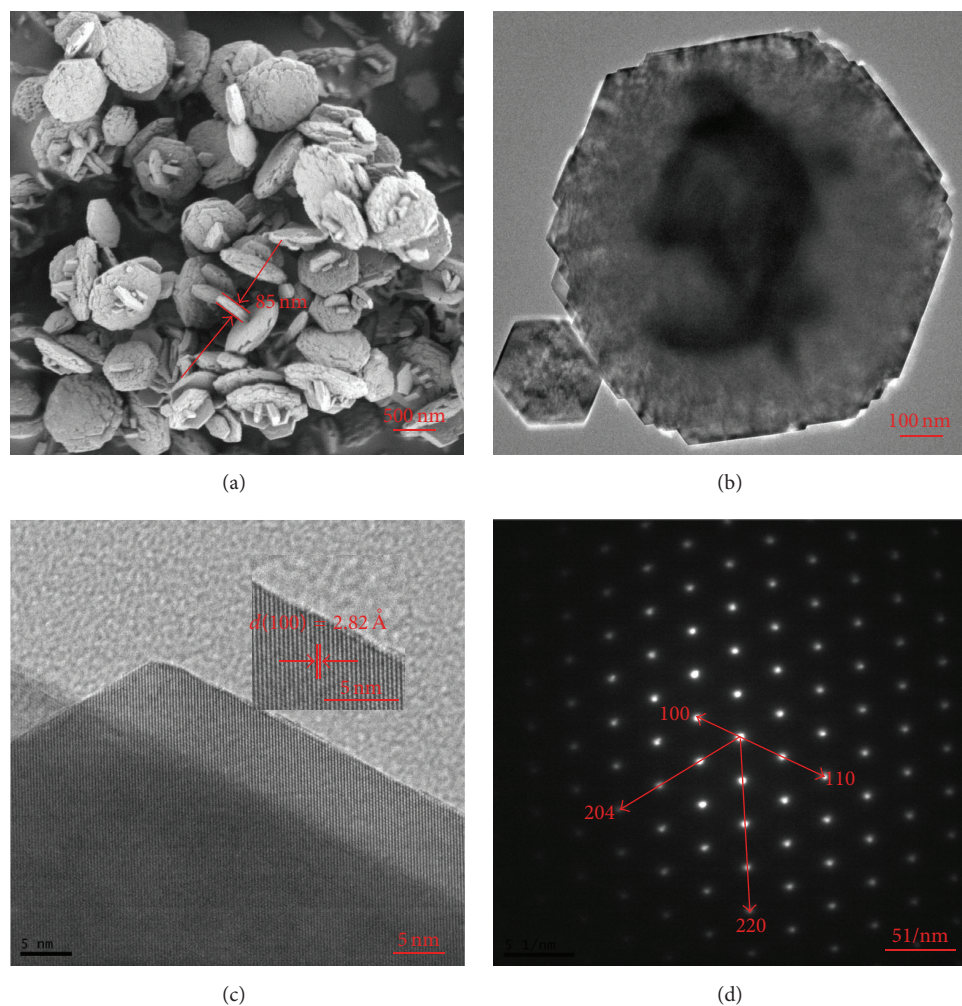


FIGURE 3: (a) SEM image of ZnO sample; (b) TEM image of ZnO sample; (c) HRTEM images of ZnO sample; (d) SAED pattern of ZnO sample.

of crystallinity, which will facilitate the alloying and dealloying processes of the reduction product of ZnO [16]. Herein, as-prepared ZnO particles with high crystallinity could be a good candidate anode for battery applications; the following electrochemical studies have confirmed this suggestion.

Figure 4 illustrates the galvanostatic discharge/charge curves of the electrode containing the hexagonal ZnO nanoplates during the initial three cycles at 0.1C. A very obvious plateau located at 0.5–0.6 V versus Li/Li⁺ appears in the first discharge curve. This plateau corresponds to the reduction process of ZnO to Zn metal ($\text{ZnO} + 2\text{Li} \rightarrow \text{Zn} + \text{Li}_2\text{O}$). Upon deep discharge, the second voltage plateau can be observed at 0.2 V versus Li/Li⁺ corresponding to the formation of lithium-zinc alloy ($x\text{Li} + \text{Zn} \rightarrow \text{Li}_x\text{Zn}$). However, in the second and subsequent discharging processes, the above plateaus are not so obvious. The synthesized ZnO nanoplate delivers first discharge capacities of 1702 mAh g^{-1} , which is much higher than theoretical value of the material, 978 mAh g^{-1} . Such result suggests extra lithium consumption

during the solid electrolyte interface (SEI) layer formation, and the formation of an SEI layer consumes a certain percentage of lithium, which is all quite common for most anode materials [8, 17], and these processes lead to a larger polarization between the reduction and oxidation peaks. After the initial activation, the slopes in discharge curves are changed, and the potential profiles in the subsequent cycles are similar in shape, indicating that the lithiation process of ZnO is reversible [18].

The galvanostatic cycling performance of the ZnO electrodes at 0.1C is depicted in Figure 5. The system achieves reversible capacity of 871 mAh g^{-1} in the second cycle and shows a good cycling stability with a reversible capacity of 368 mAh g^{-1} after 100 cycles. Furthermore, except for the initial three cycles, the coulombic efficiency of the cell is higher than 90% during the 100 cycles, which indicates a successful accommodation of the mechanical strain upon cycling by the ZnO plate-like nanostructure.

To further investigate the electrochemical properties of the ZnO electrode, the cyclability data at 1.5C were

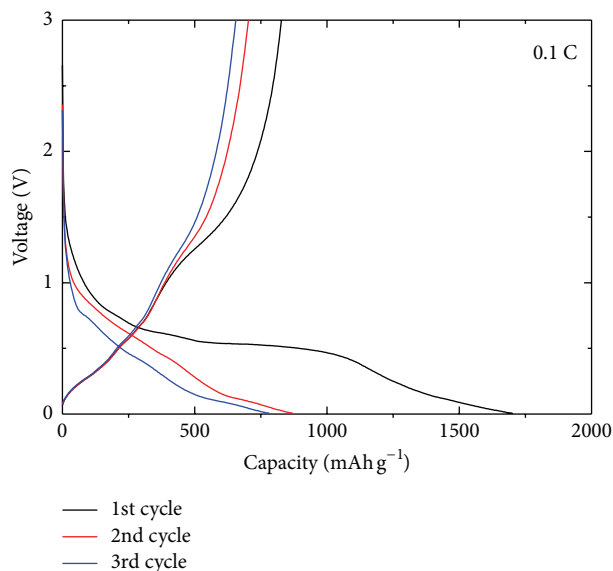


FIGURE 4: Discharge/charge profiles of lithium cell with ZnO electrode at 0.1 C.

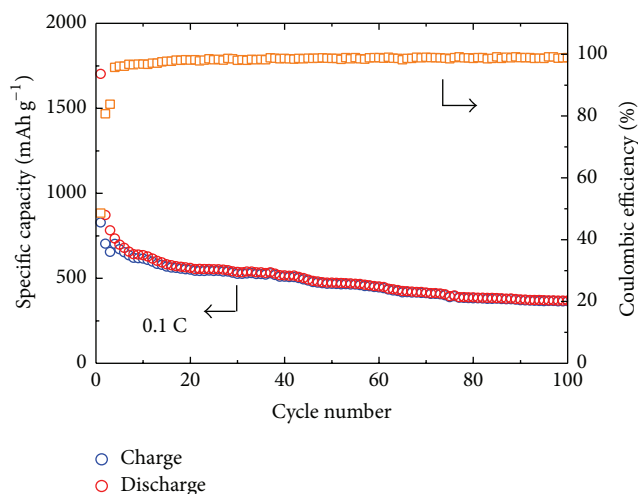


FIGURE 5: Cycle performance of lithium cell with ZnO electrode at 0.1 C.

conducted as shown in Figure 6. Although the ZnO electrode shows a limited capability of 208 mAh g^{-1} at the 2nd cycle, the cell exhibits stable cyclability with a capacity retention of 67% over 100 cycles. It could be suggested that nanoplate structure of the ZnO favors the rate capability, as further confirmed by the following study.

The rate capability results, as depicted in Figure 7, reveal the excellent high current density performance of the ZnO electrodes. After the initial activation at 0.5 C, the electrode delivers a reversible discharge capacity of 610 mAh g^{-1} at the 2nd cycle. There is a gradual capacity reduction with the current density increase, although a reversible capacity of 207 mAh g^{-1} was sustained even at 1.5 C. More importantly, when the current rate was relaxed back to a low current

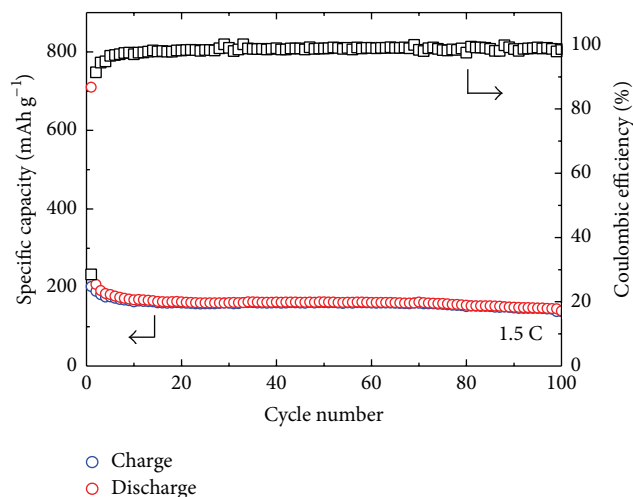


FIGURE 6: Cycle performance of lithium cell with ZnO electrode at 1.5 C.

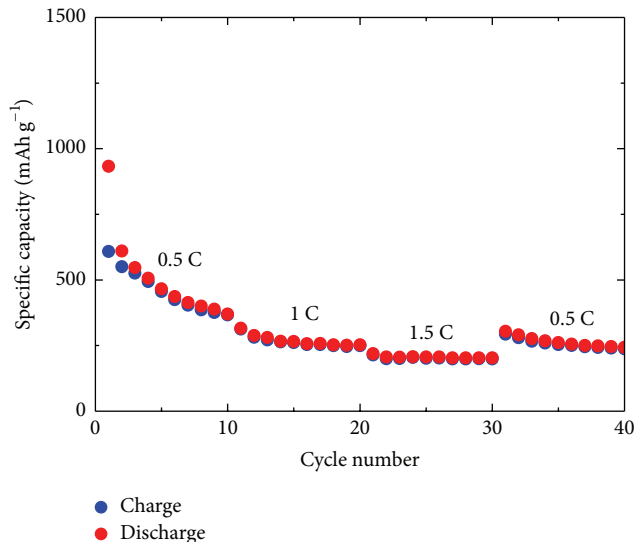


FIGURE 7: Rate capability of lithium cells with the ZnO electrode.

density of 0.5 C, the ZnO electrode recovered its capacity and continued to deliver a capacity of 304 mAh g^{-1} . This enhanced rate performance could be, again, attributed to the nanoplate structure of the material, which provides a large contact interfaces between electrode and electrolyte and short diffusion paths of lithium ions.

Figure 8 shows the SEM images of fresh and cycled ZnO electrodes. It can be seen from Figure 8 that the ZnO nanosheets merge into a large solid bulk, negatively affecting the battery performance. That well matches the fast capacity fading during the initial ten cycles.

The excellent capacity of the ZnO nanoplate is highly attractive when compared with other reported ZnO-based anode materials (Table 1). It can be observed here that the discharge capacity reaches 368 mAh g^{-1} after 100 cycles. Therefore, the good electrochemical performance of ZnO

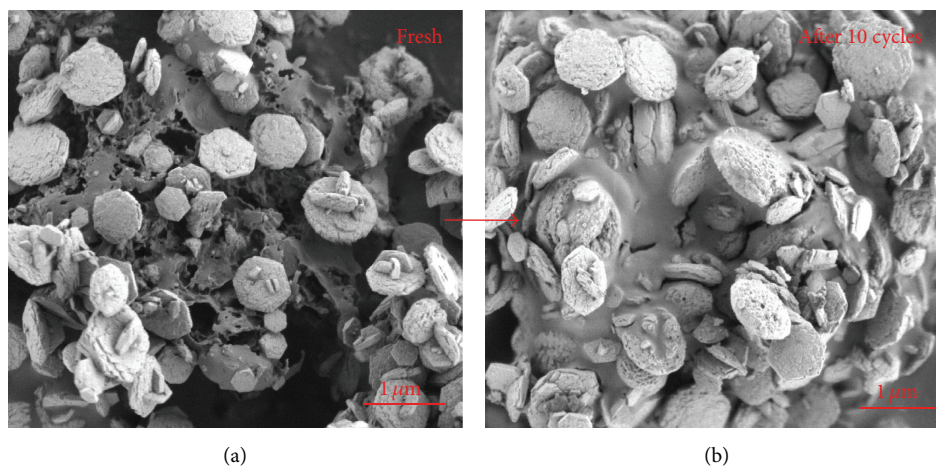


FIGURE 8: SEM images of ZnO electrodes before and after 10 charge/discharge cycles.

TABLE 1: Electrochemical performance comparison of ZnO-based anodes for lithium-ion batteries.

| Sample (morphology) | Reversible capacity (mAh g^{-1}) | Cycle number | Applied potential range (V) | Current density | Reference |
|-------------------------------------|---|--------------|-----------------------------|-------------------------|-----------|
| ZnO (radial hollow microparticles) | 320 | 100th | 0.005–3.0 | 0.2 A g^{-1} | [19] |
| ZnO (nanowire) | 252 | 30th | 0.005–3.0 | 0.12 A g^{-1} | [20] |
| ZnO (flower-like microaggregates) | 179 | 200th | 0.02–2.8 | 1 C | [21] |
| ZnO (dandelion-like nanorod arrays) | ~310 | 40th | 0–3.0 | 0.25 A g^{-1} | [22] |
| ZnO-C (flower-like nanowall arrays) | 316 | 50th | 0–3.0 | 0.5 C | [23] |
| ZnO (flower-like arrays) | 238 | 50th | 0–3.0 | 0.5 C | [23] |
| ZnO (microrod) | 150 | 50th | 0–3.0 | 0.5 A g^{-1} | [14] |
| ZnO (nanowall arrays) | ~200 | 40th | 0.02–2.0 | 0.12 A g^{-1} | [15] |
| ZnO (flower-like microparticles) | ~200 | 50th | 0.02–3.0 | 0.12 A g^{-1} | [24] |
| ZnO nanoplates | 368 | 100th | 0.005–3.0 | 0.1 C | Our work |

nanoplate makes it greatly promising for practical application.

4. Conclusions

In summary, the hexagonal ZnO nanoplates were successfully synthesized by a simple one-pot hydrothermal method. As-prepared ZnO electrode exhibited a high initial discharge capacity of 1702 mAh g^{-1} , and along with a coulombic efficiency close to 100% it maintained a reversible capacity of 368 mAh g^{-1} after 100 cycles at 0.1 C. Morphological and electrochemical data suggest that the enhanced electrochemical performance stems from the 1D plate-like structure of ZnO, which provides more active sites, shorter diffusion distances, and better accommodation for large strains upon charge-discharge operation.

Conflict of Interests

The authors declare that there is no conflict of interests regarding the publication of this paper.

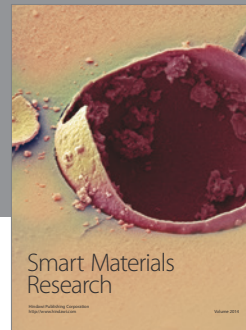
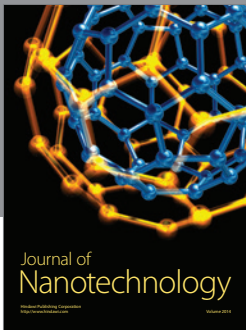
Acknowledgments

The authors acknowledge the financial support from the National Natural Science Foundation of China (Grant no. 21406052), the Program for the Outstanding Young Talents of Hebei Province (Grant no. BJ2014010), the Natural Science Foundation of Hebei Province of China (Project no. E2015202037), the Science and Technology Correspondent Project of Tianjin (Project no. 14JCTPJC00496), and research Grants from the Ministry of Education and Science of Kazakhstan (3756/GF4 and 4649/GF).

References

- [1] Y. Zhao, Y. Zhang, Z. Bakenov, and P. Chen, "Electrochemical performance of lithium gel polymer battery with nanostructured sulfur/carbon composite cathode," *Solid State Ionics*, vol. 234, pp. 40–45, 2013.
- [2] Y. Zhang, Y. Zhao, K. E. K. Sun, and P. Chen, "Development in lithium/sulfur secondary batteries," *The Open Materials Science Journal*, vol. 5, pp. 215–221, 2011.

- [3] W.-J. Zhang, "A review of the electrochemical performance of alloy anodes for lithium-ion batteries," *Journal of Power Sources*, vol. 196, no. 1, pp. 13–24, 2011.
- [4] J. B. Goodenough, "Evolution of strategies for modern rechargeable batteries," *Accounts of Chemical Research*, vol. 46, no. 5, pp. 1053–1061, 2013.
- [5] M. M. Thackeray, C. Wolverton, and E. D. Isaacs, "Electrical energy storage for transportation—approaching the limits of, and going beyond, lithium-ion batteries," *Energy & Environmental Science*, vol. 5, no. 7, pp. 7854–7863, 2012.
- [6] H. Yue, Z. Shi, Q. Wang et al., "MOF-Derived cobalt-doped ZnO@C composites as a high-performance anode material for lithium-ion batteries," *ACS Applied Materials & Interfaces*, vol. 6, no. 19, pp. 17067–17074, 2014.
- [7] M.-S. Wu and H.-W. Chang, "Self-assembly of NiO-coated ZnO nanorod electrodes with core-shell nanostructures as anode materials for rechargeable lithium-ion batteries," *Journal of Physical Chemistry C*, vol. 117, no. 6, pp. 2590–2599, 2013.
- [8] M. V. Reddy, G. V. Subba Rao, and B. V. R. Chowdari, "Metal oxides and oxyalts as anode materials for Li ion batteries," *Chemical Reviews*, vol. 113, no. 7, pp. 5364–5457, 2013.
- [9] X. Chen, Y. Huang, X. Zhang, C. Li, J. Chen, and K. Wang, "Graphene supported ZnO/CuO flowers composites as anode materials for lithium ion batteries," *Materials Letters*, vol. 152, pp. 181–184, 2015.
- [10] X. H. Huang, X. H. Xia, Y. F. Yuan, and F. Zhou, "Porous ZnO nanosheets grown on copper substrates as anodes for lithium ion batteries," *Electrochimica Acta*, vol. 56, no. 14, pp. 4960–4965, 2011.
- [11] J. Zhu, G. Zhang, S. Gu, and B. Lu, "SnO₂ nanorods on ZnO nanofibers: a new class of hierarchical nanostructures enabled by electrospinning as anode material for high-performance lithium-ion batteries," *Electrochimica Acta*, vol. 150, pp. 308–313, 2014.
- [12] G. Z. Yang, H. W. Song, H. Cui, Y. C. Liu, and C. X. Wang, "Ultrafast Li-ion battery anode with superlong life and excellent cycling stability from strongly coupled ZnO nanoparticle/conductive nanocarbon skeleton hybrid materials," *Nano Energy*, vol. 2, no. 5, pp. 579–585, 2013.
- [13] L. Jiang and L. Gao, "Fabrication and characterization of ZnO-coated multi-walled carbon nanotubes with enhanced photocatalytic activity," *Materials Chemistry & Physics*, vol. 91, no. 2–3, pp. 313–316, 2005.
- [14] X. H. Huang, J. B. Wu, Y. Lin, and R. Q. Guo, "ZnO microrod arrays grown on copper substrates as anode materials for lithium ion batteries," *International Journal of Electrochemical Science*, vol. 7, no. 8, pp. 6611–6621, 2012.
- [15] M. Ahmad, S. Yingying, H. Sun, W. Shen, and J. Zhu, "SnO₂/ZnO composite structure for the lithium-ion battery electrode," *Journal of Solid State Chemistry*, vol. 196, pp. 326–331, 2012.
- [16] L. Xiao, D. Mei, M. Cao, D. Qu, and B. Deng, "Effects of structural patterns and degree of crystallinity on the performance of nanostructured ZnO as anode material for lithium-ion batteries," *Journal of Alloys and Compounds*, vol. 627, pp. 455–462, 2015.
- [17] P. Poizot, S. Laruelle, S. Grugeon, L. Dupont, and J.-M. Tarascon, "Nano-sized transition-metal oxides as negative-electrode materials for lithium-ion batteries," *Nature*, vol. 407, no. 6803, pp. 496–499, 2000.
- [18] J. Yan, G. Wang, H. Wang et al., "Preparation and electrochemical performance of bramble-like ZnO array as anode materials for lithium-ion batteries," *Journal of Nanoparticle Research*, vol. 17, no. 1, pp. 1–10, 2015.
- [19] G. Yuan, G. Wang, H. Wang, and J. Bai, "Synthesis and electrochemical investigation of radial ZnO microparticles as anode materials for lithium-ion batteries," *Ionics*, vol. 21, no. 2, pp. 365–371, 2014.
- [20] J. Wang, N. Du, H. Zhang, J. Yu, and D. Yang, "Layer-by-layer assembly synthesis of ZnO/SnO₂ composite nanowire arrays as high-performance anode for lithium-ion batteries," *Materials Research Bulletin*, vol. 46, no. 12, pp. 2378–2384, 2011.
- [21] V. Cauda, D. Pugliese, N. Garino et al., "Multi-functional energy conversion and storage electrodes using flower-like Zinc oxide nanostructures," *Energy*, vol. 65, pp. 639–646, 2014.
- [22] H. Wang, Q. Pan, Y. Cheng, J. Zhao, and G. Yin, "Evaluation of ZnO nanorod arrays with dandelion-like morphology as negative electrodes for lithium-ion batteries," *Electrochimica Acta*, vol. 54, no. 10, pp. 2851–2855, 2009.
- [23] Z. Wu, L. Qin, and Q. Pan, "Fabrication and electrochemical behavior of flower-like ZnO-CoO-C nanowall arrays as anodes for lithium-ion batteries," *Journal of Alloys and Compounds*, vol. 509, no. 37, pp. 9207–9213, 2011.
- [24] M. Ahmad, S. Yingying, A. Nisar et al., "Synthesis of hierarchical flower-like ZnO nanostructures and their functionalization by Au nanoparticles for improved photocatalytic and high performance Li-ion battery anodes," *Journal of Materials Chemistry*, vol. 21, no. 21, pp. 7723–7729, 2011.



Hindawi

Submit your manuscripts at
<http://www.hindawi.com>

